

F-Block N-Heterocyclic Carbene Complexes

Polly L. Arnold* and Ian J. Casely

School of Chemistry, University of Edinburgh, Joseph Black Building, West Mains Road, Edinburgh, EH9 3JJ, U.K.

Received November 13, 2008

Contents

1. Introduction	3599
1.1. The Place for This Review	3599
1.2. Past Reviews	3599
1.3. Range of This Review	3599
2. Complexes of Group 3	3600
2.1. Scandium-NHC Complexes	3600
2.2. Yttrium-NHC Complexes	3600
2.3. Lanthanum-NHC Complexes	3603
3. Complexes of the Lanthanoids	3603
3.1. Cerium(III)-NHC Complexes	3603
3.2. Cerium(IV)-NHC Complexes	3604
3.3. Neodymium-NHC Complexes	3604
3.4. Samarium(II)-NHC Complexes	3606
3.5. Samarium(III)-NHC Complexes	3606
3.6. Europium(III)-NHC Complexes	3607
3.7. Mid-lanthanide-NHC Complexes	3607
3.8. Holmium(III)-NHC Complexes	3607
3.9. Erbium(III)-NHC Complexes	3607
3.10. Ytterbium(II)-NHC Complexes	3607
3.11. Ytterbium(III)-NHC Complexes	3608
3.12. Lutetium(III)-NHC Complexes	3608
4. Actinide-NHC Complexes	3608
4.1. Uranium(III)-NHC Complexes	3608
4.2. Uranium(IV)-NHC Complexes	3609
4.3. Uranium(VI)-NHC Complexes	3610
5. Abbreviations	3610
6. References	3610

1. Introduction

1.1. The Place for This Review

The use of N-heterocyclic carbenes as ligands is a rapidly expanding field, and exciting compounds and catalytic uses are being described for their metal complexes with increasing frequency. Since the first examples of metal carbene complexes appeared in the literature, it has been appreciated that the σ -donor carbene can bind effectively to more electro-positive metals despite its soft character. The number of group 3, lanthanide, and actinide carbene complexes has steadily grown over the last five years in particular, along with the range of applications for these complexes in the activation of small, inert, molecules and as homogeneous catalysts. This review attempts to summarize the entire

activity in organolanthanide, actinide, and group 3 chemistry of N-heterocyclic carbenes that has been published to date.

1.2. Past Reviews

A thematic issue of *Chemical Reviews* entitled “Frontiers in Lanthanide Chemistry” was published in 2002.¹

More recent reviews on organometallic lanthanide chemistry have focused on very particular areas, for example, the synthesis of cationic organometallic group 3 and lanthanide complexes,² nonmetallocene alkene polymerization catalysts,³ and nonmetallocene hydrides.⁴ Structurally characterized lanthanide alkoxide and aryloxide complexes have been discussed very recently in an excellent review by Boyle and Ottley.⁵ Lanthanide amide complexes and their suitability as transamination catalysts have also been surveyed.⁶

Some highlights of molecular uranium chemistry from the past decade were published in 2006,⁷ and the scope of reduction chemistry by uranium(III) compounds was surveyed in the same year.⁸ The homogeneous catalytic aspects of organometallic uranium chemistry that are already known,⁹ and may be possible in the future,¹⁰ have also been reviewed.

The number of reviews on carbene chemistry is growing rapidly, but this is in line with the widespread interest in their use as ligands for a variety of metals. The most recent general review on metal-NHC complexes was published in the summer of 2008.¹¹ We published a brief survey of our work in the area in 2006.¹² We also reviewed the use of anionic tethered NHC ligands for metal chemistry in general¹³ and the potential for the carbene to bind through a backbone carbon instead of the expected carbene carbon to metals across the periodic table.¹⁴

Two books should also be mentioned in the context of reviewing the coordination and organometallic chemistry of the lanthanides and actinides—Cotton’s concise textbook on lanthanide and actinide chemistry,¹⁵ and the more comprehensive five-volume work covering the actinides and trans-actinides.¹⁶

Finally, an award article has been written by Evans that challenges the academic community to question scientific assumptions, providing examples of new ways to accomplish redox chemistry with f-block complexes.¹⁷

1.3. Range of This Review

For this review, we have endeavored to include every single compound of the metals of group 3, the lanthanides, and actinides that contains an N-heterocyclic carbene, whether metal-bound or not. Where relevant, we have also mentioned details of the characterization and/or reactivity of a given compound.

* Telephone: (+44) 131 650 5429. Fax: (+44) 131 650 6453. E-mail: Polly.Arnold@ed.ac.uk.



Polly L. Arnold was born in London, U.K., in July 1972. She obtained a B.A. from Oxford in 1994 and a D.Phil. in 1997 from Sussex, supervised by Professor Geoff Cloke. She was awarded a Fulbright Scholarship for postdoctoral research with Professor Kit Cummins at MIT and returned to the U.K. to take up a lectureship at the University of Nottingham in 1999. She held an EPSRC Advanced Research Fellowship position between 2000 and 2005 and was promoted to Reader in 2006. She moved to the University of Edinburgh as an EaStCHEM fellow in April 2007. She was awarded the Bessel Prize by the Humboldt Foundation in 2007, after being taught some useful German phrases by Ian. She received the Chancellor's prize of the University of Edinburgh and the RSC Sir Edward Frankland Prize Lectureship in 2008. Her research is focused on the synthesis of early transition metal and f-block inorganometallic complexes and the study of their bonding, small molecule activation chemistry, and catalytic applications.



Ian J. Casely was born in October 1981 and grew up in Grimsby, U.K. He studied chemistry at Imperial College London, which included a one year industrial placement at Boehringer Ingelheim Pharma K.G., Germany, where he immersed himself in German culture and learned to ski. Following this, he completed his M.Sci. research project on group 2 hydroamination catalysis with Dr. Mike Hill in 2005. His Ph.D. research on electropositive metal N-heterocyclic carbene complexes began at the University of Nottingham with Polly Arnold and concluded successfully at the University of Edinburgh in March 2009. He recently got married and will shortly start postdoctoral research.

2. Complexes of Group 3

2.1. Scandium-NHC Complexes

Scandium NHC's were only recently reported by Cui et al. (**1** and **2** in Figure 1).¹⁸ Both complexes were synthesized from the indenyl- or fluorenyl-functionalized free carbene, HL in Figure 1 (HL = C₉H₇CH₂CH₂(NCHCCHN)C₆H₂Me₃-2,4,6 and C₁₃H₇CH₂CH₂(NCHCCHN)C₆H₂Me₃-2,4,6, respectively), made from a single deprotonation of the corresponding imidazolium bromide precursor [H₂L]Br with LiCH₂SiMe₃. Subsequent treatment with the scandium tris-

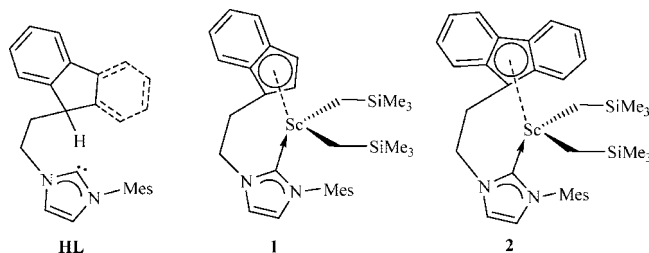


Figure 1.

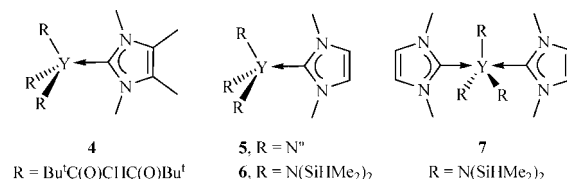
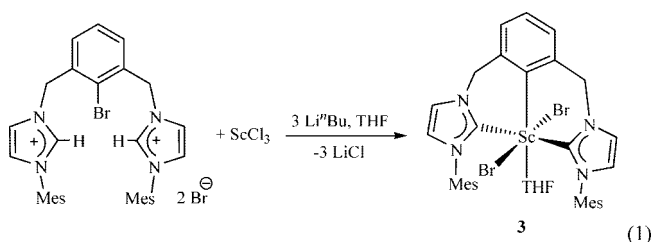


Figure 2.

alkyl Sc(CH₂SiMe₃)₃(THF)₂ removed the remaining acidic cyclopentadienyl proton to furnish the indenyl-NHC scandium bis-alkyl complex **1** and the fluorenyl-substituted derivative **2**, respectively. The C_{carbene} resonances in the ¹³C NMR spectra for both complexes of $\delta = 188.0$ and 187.6 ppm, respectively, suggest the NHC is bound to the metal center. Structural characterization revealed a tetrahedral geometry at the scandium center with Sc–C_{carbene} bond lengths of 2.350(3) and 2.343(4) Å, respectively.

The same authors have subsequently reported a scandium complex of a tridentate CCC-pincer bis-carbene ligand, **3** in eq 1, as the dibromide THF solvate.¹⁹ The synthesis of this complex is unusual, as the dibromide salt of the ligand precursor was deprotonated *in situ* with 3 equiv of Li^{*i*}Bu in the presence of ScCl₃; from this the scandium dibromide ligand adduct **3** was isolated instead of the expected dichloride, (eq 1). The mechanism associated with this process remains unknown. Complex **3** was structurally characterized by a single crystal X-ray diffraction study; the molecular structure contains a square-bipyramidal geometry scandium cation, the tridentate ligand adopts a pseudo-*meridional* conformation with average Sc–C_{carbene} bond lengths of 2.390 Å. The ¹³C NMR spectrum contains a C_{carbene} resonance of $\delta = 193.1$ ppm, which lies within the expected high-frequency region for a metal-bound NHC.

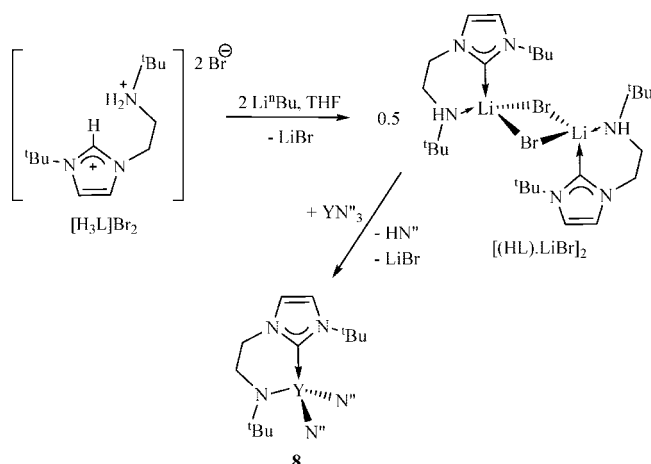


2.2. Yttrium-NHC Complexes

The first example of a yttrium-NHC complex was reported by Arduengo et al. in 1994, as the monoadduct [Y(thd)₃(C{NMeCMe}₂)₂], **4** in Figure 2 (where thd = tetramethylheptanedioate and N'' = N(siMe₃)₂).²⁰ The ¹³C NMR spectrum showed a C_{carbene} resonance at $\delta = 199.4$ ppm as a doublet, due to coupling to the $I = 1/2$ yttrium center, with a coupling constant of ¹J_{YC} = 33 Hz.

A later report from Anwender et al. examined monoadduct formation of an NHC with yttrium tris-amido compounds.²¹ They initially examined the complex [YN''₃(C{NMeCH}₂)₂]

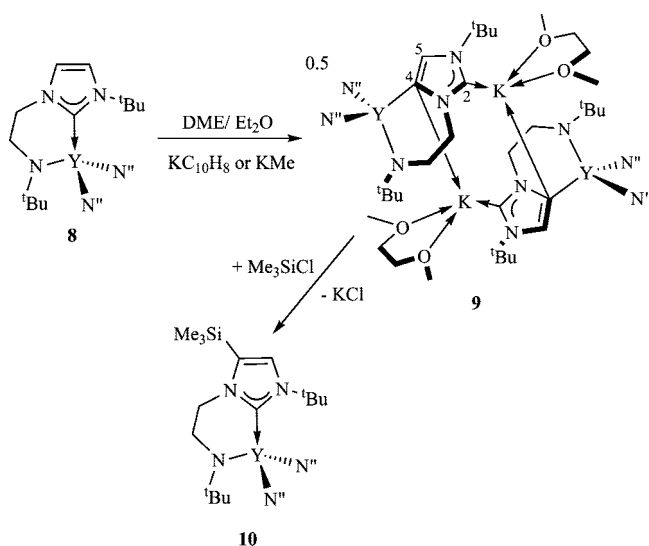
Scheme 1



(5), Figure 2, and characterized it by IR spectroscopy, elemental analysis, and NMR spectroscopy, although the C_{carbene} resonance in the ^{13}C NMR spectrum was not reported. They then investigated the mono-NHC complex $[Y(N\{SiHMe_2\}_2)_3(C\{NMeCH\}_2)]$ (**6**) and the bis-NHC complex $[Y(N\{SiHMe_2\}_2)_3(C\{NMeCH\}_2)_2]$ (**7**), both shown in Figure 2, which were formed by treatment of the corresponding bis-THF adduct $Y(N\{SiHMe_2\}_2)_3(THF)_2$ with one or two equivalents of the free carbene, respectively. The ^{13}C NMR spectrum for **6** shows a C_{carbene} resonance at $\delta = 190.3$ ppm, resonating as a doublet $^1J_{YC} = 49.6$ Hz, which is larger than the value of 33 Hz previously reported and indicates a strong interaction between the yttrium and carbene groups in solution. The C_{carbene} resonance in **7** was observed at $\delta = 194.0$ ppm, although no coupling constant was given. Both complexes were structurally characterized. Complex **6** crystallizes with two crystallographically independent molecules in the unit cell and the geometry at the yttrium center is distorted tetrahedral, with an out-of-plane bending “pitch” of the NHC plane from the Y-NHC plane of 8.7° , considerably smaller than those observed in group one metal complexes. The five-coordinate yttrium center in **7** is pseudotrigonal bipyramidal, with the two NHC ligands diametrically opposed in this more sterically encumbered complex. The $Y-C_{\text{carbene}}$ bond lengths of 2.55(1) and 2.560(9) Å in **6** and 2.648(8) and 2.671(9) Å in **7** are consistent with the higher coordination number in the latter complex.

The first N-functionalized NHC yttrium complex was reported by our group, **8** in Scheme 1, and was synthesized through treatment of YN'''_3 with an equivalent of the lithium bromide adduct of the amine-carbene ligand precursor $[(HL) \cdot LiBr]_2$, accompanied by loss of hexamethyldisilazane.²² A single crystal X-ray diffraction study revealed the geometry at the yttrium center as pseudotetrahedral with a $Y-C_{\text{carbene}}$ bond length of 2.501(5) Å. The ^{13}C NMR spectrum displayed a yttrium-coupled C_{carbene} resonance as a doublet at $\delta = 186.3$ ppm, with a coupling constant of $^1J_{YC} = 54.7$ Hz, which was the largest yet reported value for a yttrium-NHC or even an yttrium-alkyl complex at the time. A series of preliminary competition studies with potential donor ligands were undertaken with **8** in order to probe the lability of the Y-NHC bond. The addition of 1 equiv of THF, Et_2O , PPh_3 , or Me_3NO showed no reaction, but TMEDA or $OPPh_3$ successfully displaced the NHC group. These reactions were monitored by ^{13}C NMR spec-

Scheme 2



troscopy, with the last two reagents resulting in the loss of $^1J_{YC}$ coupling and therefore the Y-NHC bond (*vide infra*).

Following these investigations, complex **8** was found to be an excellent bifunctional catalyst for the ring-opening polymerization of *rac*-lactide, producing highly heterotactic poly(*rac*-lactide) with low polydispersity. The bifunctional nature of the catalyst resulted from the lactide binding to the Lewis acidic yttrium center, after which the labilized NHC functioned as a Lewis base to ring-open the monomer by a nucleophilic mechanism.²³

Subsequently, our group reported that the treatment of **8** with potassium naphthalenide in DME/diethyl ether at $-78^\circ C$ afforded complex **9**, Scheme 2, formally as the product of deprotonation and subsequent migration of the C2 carbene from yttrium to the incorporated potassium cation, and this represents the first example of a C,C-bridged NHC complex.²⁴ The ^{13}C NMR spectrum shows C2 and C4 carbene resonances at $\delta = 199.2$ and 167.5 ppm, respectively, with the latter of these manifesting as a yttrium coupled doublet, $^1J_{YC} = 62$ Hz. This is the largest coupling constant so far reported and indicates a very strong interaction between yttrium and the C4 carbene. An X-ray structural determination revealed that **9** is dimeric in the solid state, with each four coordinate yttriate center being N-bound to two N''' ligands, one amide-N of the NHC tether, and the newly formed C4 carbanion of the NHC backbone. The $Y-C4$ bond length of 2.447(2) Å is significantly shorter than the $Y-C2$ bond length in **8**, in agreement with the large observed $^1J_{YC}$ coupling constant, and is at the short end of the $Y-C$ single σ -bond range. Changing the reducing agent to KC_8 resulted in no reaction. As complex **9** is the product of a deprotonation reaction, treatment of **8** with a base was investigated. Although the use of KN''' resulted in only trace amounts of **9** being isolated, when KMe was used as the deprotonating reagent, the product could be isolated in high yield, 82%.

Complex **9** can be quenched with electrophiles, such that upon addition of Me_3SiCl , the regioselectively C4-silylated complex **10** can be isolated in quantitative yield, with concomitant elimination of KCl (Scheme 2). The ^{13}C NMR spectrum shows a lower field chemical shift for the $Y-C2$ resonance at $\delta = 172.7$ ppm, which is again yttrium-coupled, $^1J_{YC} = 55.8$ Hz—a particularly large coupling constant, possibly signifying a very strong σ -interaction between the two atoms.

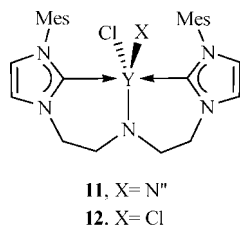


Figure 3.

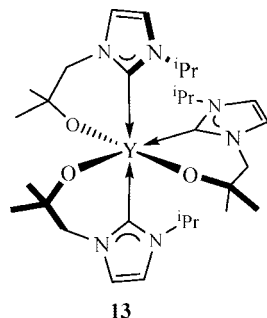


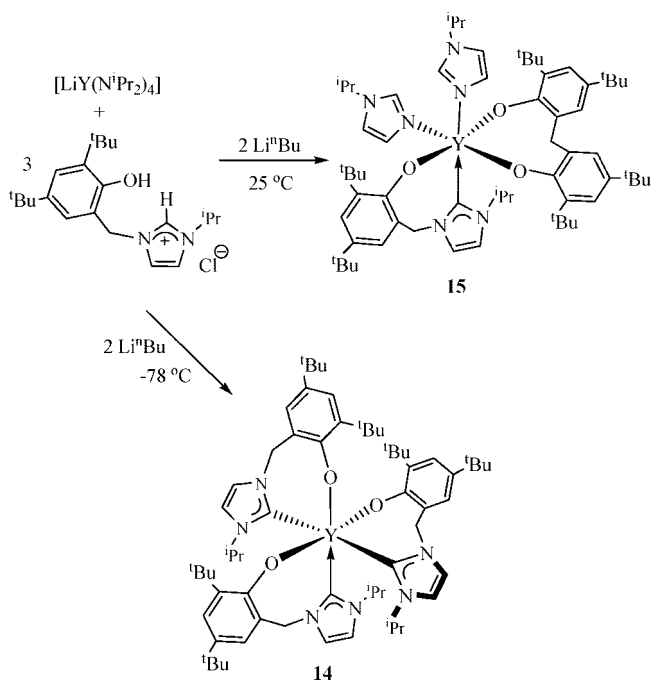
Figure 4.

The yttrium complex **11** (Figure 3) was synthesized from YN''_3 and 1 equiv of the lithium chloride adduct of the aminodicarbene ligand, $[(\text{LiCl})_3\text{HL}]$, and the complexation of yttrium was again confirmed by ^{13}C NMR spectroscopy, which showed a yttrium coupled doublet at $\delta = 194.3$ ppm ($^1J_{\text{YC}} = 48$ Hz).²⁵ This coupling is comparable to that of other yttrium-NHC complexes but is smaller than that observed in the previously discussed bidentate amidocarbene complexes such as **8**. The molecular structure of **11** shows $\text{Y}-\text{C}_{\text{carbene}}$ bond lengths of 2.574(3) and 2.565(3) Å, which lie within reported values, although they are longer than those observed in the bidentate amidocarbene complexes. The geometry at the yttrium center is distorted trigonal bipyramidal, with the tridentate ligand occupying a *meridional* configuration about the metal.

Complex **11** could be reliably isolated as the only product from this reaction, except upon one occasion when the dichloride **12** was isolated. All attempts at a rational synthesis of this complex from $\text{YCl}_3(\text{THF})_3$ failed. This complex was characterized by NMR spectroscopy and elemental analysis, and it showed a yttrium coupled $\text{C}_{\text{carbene}}$ resonance at $\delta = 192.8$ ppm in the ^{13}C NMR, with a coupling constant $^1J_{\text{YC}} = 47$ Hz. The lability of the $\text{Y}-\text{NHC}$ bond was investigated *via* a series of competition experiments with triphenyl- and trimethyl-phosphine oxides. Although reactions of **11** only resulted in decomposition products, those of complex **12** yielded tractable precipitates from benzene which were formulated as the simple triphenyl- and trimethylphosphine oxide adducts. Both complexes showed yttrium coupled $\text{C}_{\text{carbene}}$ resonances in the ^{13}C NMR spectra at $\delta = 193.0$ ppm ($^1J_{\text{YC}} = 38$ Hz) for the remaining bound carbene, indicating that only products of one NHC displacement could be isolated in these systems.

Our group has very recently reported the synthesis of complex **13** (Figure 4) through treatment of $\text{YCl}_3(\text{THF})_3$ with 3 equiv of the corresponding potassium ligand salt, $[\text{KL}]$. Solutions of this complex exhibit a ^{13}C NMR spectrum with a $\text{C}_{\text{carbene}}$ resonance at $\delta = 197.3$ ppm, at the high-frequency end of reported carbene chemical shifts, and with a $^1J_{\text{YC}}$ coupling constant of 31 Hz.²⁶ The solid state structure of **13** revealed the three *meridionally*-disposed ligands form a pseudo-octahedral geometry about the yttrium center. Al-

Scheme 3



though the complex is not C_3 -symmetric according to crystallography, at room temperature, only one set of ligand resonances was measured in the ^1H NMR spectrum. However, cooling a solution of **13** revealed the magnetic inequivalence of the three ligands, confirming that the structurally characterized single crystal was indeed representative of the bulk. The average $\text{Y}-\text{C}_{\text{carbene}}$ bond length of 2.588(12) Å is comparable to that of previously discussed examples. A computational study in search of evidence for early metal NHC π -backbonding interactions, through comparison of d^0 **13** and the d^1 Ti^{III} analogue, TiL_3 ,²⁷ concluded that the observed shortening of the $\text{Ti}-\text{C}$ versus the $\text{Y}-\text{C}$ bonds was most likely due to the increased electrostatic interaction caused by the smaller titanium center and not a π -backbonding interaction.

Shen et al. have reported the synthesis of aryloxy-functionalized NHC yttrium complexes, **14** and **15** in Scheme 3, through treatment of $[\text{LiY}(\text{N}^i\text{Pr}_2)_4]$ with the corresponding ligand chloride salt and Li^nBu in a 1:3:2 molar ratio.²⁸ Complex **14** was isolated when the reaction was conducted at -78 °C. The ^{13}C NMR spectrum of **14** contained a very high-field $\text{C}_{\text{carbene}}$ resonance at $\delta = 199.9$ ppm, although the magnitude of the expected yttrium coupling has not been reported. An X-ray diffraction study revealed the geometry at the yttrium center to be distorted octahedral with an average $\text{Y}-\text{C}_{\text{carbene}}$ bond length of 2.621(3) Å, which is longer than that in other $\text{Y}-\text{NHC}$ examples.

When the same reaction is conducted at room temperature, the mono-NHC yttrium complex **15**, bearing a methylene-bridged bis-aryloxo ligand instead of the expected ethyl-bridge, is isolated. This complex has a $\text{C}_{\text{carbene}}$ resonance at $\delta = 198.4$ ppm in the ^{13}C NMR spectrum. The molecular structure shows a pseudo-octahedrally coordinated yttrium cation with a $\text{Y}-\text{C}_{\text{carbene}}$ bond length of 2.576(5) Å, closer to that in other examples. The mechanism involved in the formation of **15** remains unproven, although a reaction pathway proceeding *via* hydrogen transfer from the phenol to the carbene center, breaking the benzylic $\text{N}-\text{C}$ bond, was proposed. This then requires an attack of the unsaturated

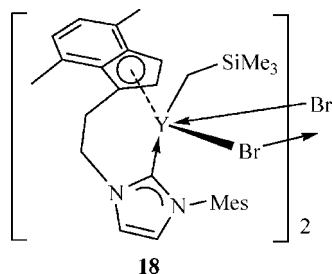


Figure 5.

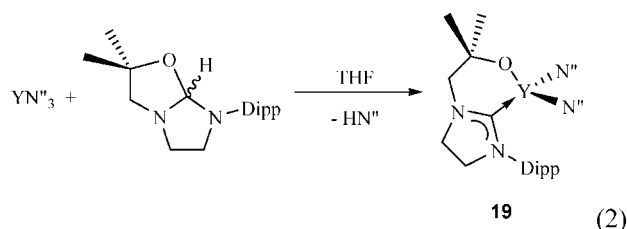
ligand fragment by a metal-bound amido group to release a tertiary amine byproduct to allow the methylene-bridge coupled phenol to form.

Yttrium bis-alkyl analogues of complexes **1** and **2** (Figure 1) bearing indenyl- and fluorenyl-functionalized NHC ligands were reported at the same time by Cui et al., such that *in situ* deprotonation of the corresponding imidazolium bromide precursor with $\text{LiCH}_2\text{SiMe}_3$, followed by addition of $[\text{Y}(\text{CH}_2\text{SiMe}_3)_3(\text{THF})_2]$, furnished the indenyl-functionalized complex $[(\text{Ind-NHC})\text{Y}(\text{CH}_2\text{SiMe}_3)_2]$ (**16**) and the fluorenyl-functionalized complex $[(\text{Flu-NHC})\text{Y}(\text{CH}_2\text{SiMe}_3)_2]$ (**17**), respectively ($\text{Ind-NHC} = \text{C}_9\text{H}_6\text{CH}_2\text{CH}_2(\text{NCHCCHN})\text{C}_6\text{H}_2\text{Me}_3$ -2,4,6, $\text{Flu-NHC} = \text{C}_{13}\text{H}_8\text{CH}_2\text{CH}_2(\text{NCHCCHN})\text{C}_6\text{H}_2\text{Me}_3$ -2,4,6).¹⁸ Both indenyl and fluorenyl complexes exhibited yttrium-coupled $\text{C}_{\text{carbene}}$ resonances in the ^{13}C NMR spectra at $\delta = 191.2$ ppm ($^1J_{\text{YC}} = 46.0$ Hz) and $\delta = 190.8$ ppm ($^1J_{\text{YC}} = 45.8$ Hz), respectively, and in the solid state the former was proven to adopt a tetrahedral geometry at the yttrium center with a $\text{Y}-\text{C}_{\text{carbene}}$ bond length of $2.501(3)$ Å. Both of these complexes were found to be active catalysts for the 3,4-selective living polymerization of isoprene.

Prior to these Ind-NHC and Flu-NHC reports, Danopoulos et al. had reported early transition metal adducts of related ligands.²⁹ They subsequently reported an yttrium alkyl complex supported by the indenyl-functionalized NHC ligand, $[1-(4,7\text{-Me}_2\text{-C}_9\text{H}_4)\text{CH}_2\text{CH}_2(\text{C}\{\text{NCHCCHN}(2,4,6\text{-Me}_3\text{-C}_6\text{H}_2)\})\text{Y}(\text{CH}_2\text{SiMe}_3)(\mu\text{-Br})_2]$ (**18**) in Figure 5, which despite being inaccessible from salt elimination routes was successfully synthesized by treatment of $[\text{Y}(\text{CH}_2\text{SiMe}_3)_3(\text{THF})_2]$ with 1 equiv of the corresponding imidazolium bromide ligand precursor.³⁰ Complex **18** decomposes over time in solution, such that no ^{13}C NMR spectra could be obtained, but solid state analysis revealed the molecular structure as a centrosymmetric bromide-bridged dimer with the yttrium center in a square-pyramidal geometry and a $\text{Y}-\text{C}_{\text{carbene}}$ bond length of $2.547(5)$ Å.

We have very recently reported the first example of an early metal complex bearing a saturated backbone NHC ligand, **19** in eq 2.³¹ Complex **19** was synthesized by treatment of YN''_3 with the bicyclic carbene-alcohol adduct proligand $[\text{OCMe}_2\text{CH}_2(1\text{-CH}\{\text{NCH}_2\text{CH}_2\text{NDipp}\})]$ and was readily identified by the $^1J_{\text{YC}} = 42$ Hz coupling of the $\text{C}_{\text{carbene}}$ resonance at $\delta = 216.3$ ppm in the ^{13}C NMR spectrum. This is a higher frequency chemical shift than that observed for unsaturated yttrium-NHC complexes, which typically fall in the range $\delta = 180\text{--}200$ ppm. The ^1H NMR spectrum is also indicative of ligand complexation, as coupling multiplet patterns of the magnetically inequivalent CH_2 groups are simplified upon breaking of the bicyclic ring system. Structural analysis revealed the geometry at the yttrium center to be pseudotetrahedral, with a long $\text{Y}-\text{C}_{\text{carbene}}$ bond length of $2.599(2)$ Å; a consequence of the sterically demanding Dipp substituent. Although long when compared to those of

other unsaturated Y-NHC complexes, this distance is not outside the range of σ -bonded Y-alkyl bond lengths.



2.3. Lanthanum-NHC Complexes

The only reported lanthanum-NHC complex is the simple adduct $[\text{LaN}''_3(\text{C}\{\text{NMeCH}\}_2)]$ (**20**), which was characterized by IR and NMR spectroscopies and elemental analysis. No further details have been reported.²¹

3. Complexes of the Lanthanoids

3.1. Cerium(III)-NHC Complexes

The first Ce-NHC complexes, reported by our group in 2005,³² contained an anionic, amido-functionalized NHC ligand. Thus, complex **21** (Figure 6) was synthesized *via* a transamination reaction between CeN''_3 and 0.5 equiv of the amine-NHC lithium bromide adduct $[(\text{HL})\cdot\text{LiBr}]_2$, shown in Scheme 1. Structural analysis showed the complex to possess a $\text{Ce}-\text{C}_{\text{carbene}}$ bond length of $2.670(2)$ Å in the solid state, comparable to that seen in the four-coordinate U^{III} NHC complex **69**, and long $\text{Ce}-\text{N}_{\text{silylamide}}$ bond lengths of $2.418(2)$ and $2.404(2)$ Å, a consequence of the sterically congested metal center. On one occasion, complex **22** was isolated from the above reaction, which subsequently proved to be unrepeatable, and formed *via* a ligand exchange reaction between the lithium bromide eliminated from the starting material and the product **21**. Structural analysis of **22** revealed a slightly longer $\text{Ce}-\text{C}_{\text{carbene}}$ bond length of $2.699(2)$ Å than that observed in **21**, possibly attributable to the larger coordination number of the metal center. The $\text{Ce}-\text{N}_{\text{silylamide}}$ bond length of $2.376(2)$ Å is again toward the higher end of reported values, although shorter than that in **21**, and the two $\text{Ce}-\text{Br}$ bond lengths of $3.026(2)$ and $3.056(2)$ Å are predictably long due to their bridging nature.

Although complex **22** is a potentially useful starting point to investigate further metathesis chemistry, the synthesis was not ideal and obviated its possible utility. As the bromide originated from the LiBr incorporated in the starting material, **21** was treated with LiI in a rational route to target the iodide analogue, **23**. An X-ray diffraction study of **23** revealed it to be isomorphous with **22**.

Treatment of **21** with 1 equiv of Me_3SiI afforded the regioselectively C4-silylated iodide-bridged dimer **24**, and structural characterization shows a $\text{Ce}-\text{C}_{\text{carbene}}$ bond length

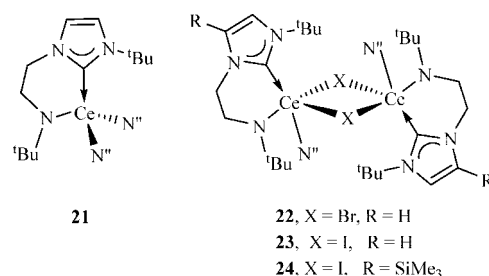


Figure 6.

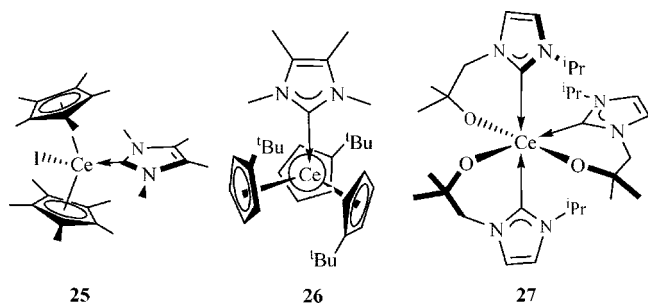


Figure 7.

of 2.728(8) Å; it is isostructural with the neodymium compound **31**, below.

Complexes **22–24** are rare examples of heteroleptic lanthanide complexes of the type $\text{LnL}^1\text{L}^2\text{L}^3$, due to the prevalence of redistribution reactions for these metals with no orbital constraints on their bonding. The isolation of such kinetically inert heteroleptic complexes is normally limited to the smaller, heavier, lanthanides.

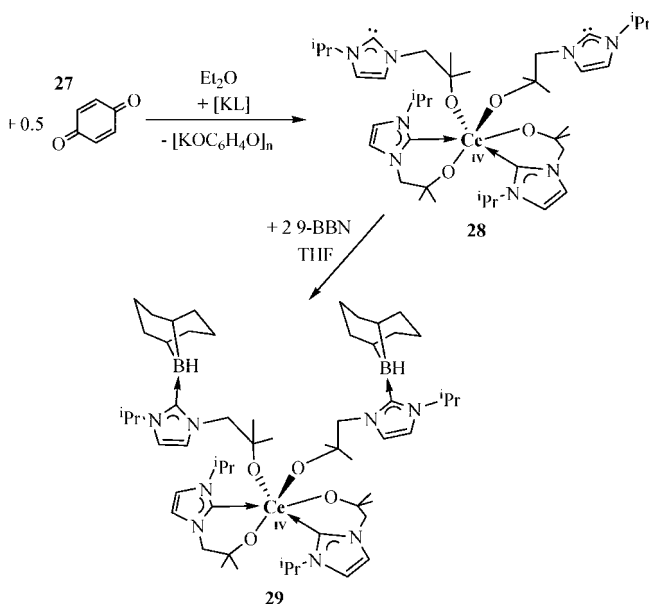
Soon after the report of complexes **21–24**, Ephritikhine published complexes **25** and **26** (Figure 7).³³ These are both adducts of the simplest two-electron donor NHC, C(NMeC-Me)₂, and can be synthesized by mixing the free NHC with the corresponding Ce^{III} starting material. Structural characterization of both **25** and **26** confirmed the pseudotetrahedral geometry at each metal center and Ce–C_{carbene} bond lengths of 2.724(4) and 2.768(5) Å, respectively, which are longer than those in **21** (in agreement with the higher coordination number at Ce).

We have subsequently reported that treatment of CeI₃(THF)₄ with three equivalents of the potassium salt of an alkoxy-functionalized NHC [KL], K[OCMe₂CH₂(1-C{NC-HCHNPrⁱ})], readily affords the cerium tris-alkoxy-NHC complex, **27** in Figure 7.³⁴ Although not yet structurally characterized, the paramagnetically shifted ligand resonances observed in the ¹H NMR spectrum of **27** are sharp and spread over a relatively small chemical shift range, suggesting a high-symmetry structure. The solution magnetic susceptibility was also determined as 2.21 μ_B at 300 K; the typical range for Ce^{III} complexes is 1.8–2.5 μ_B.

3.2. Cerium(IV)-NHC Complexes

The only examples of tetravalent cerium NHC complexes have been recently reported by our group.³⁴ The oxidation of **27** with 1 equiv of benzoquinone affords the tetravalent cerium-NHC complex **28** (Scheme 4), which is a product of both the desired oxidation and also a ligand redistribution. The inclusion of an additional equivalent of [KL] results in increased yields of **28**, since none of the starting material **27** is sacrificed as a source of L. This oxidation to form **28** can also be effected by XeF₂ and [Fe(Cp)₂][OTf], albeit in considerably lower yields. Due to the diamagnetic nature of Ce^{IV} complexes, the C_{carbene} resonance can be observed in the ¹³C NMR spectrum at δ = 212.6 ppm, and the ¹H NMR spectrum displays one set of ligand resonances which is commensurate with a fast fluxional process between the free and bound carbenes on the NMR time scale. In light of this, a low temperature VT NMR experiment was conducted; at 230 K the ¹H resonances decoalesce, whereas at 198 K three sets of ligand resonances can be observed in a 2:1:1 ratio. This implies fast motion for the two pendant carbenes on the NMR time scale and a sterically congested metal center

Scheme 4



imparting differing magnetic environments on the protons of the two bidentate ligands. Single crystal X-ray structural characterization (150 K) revealed the geometry at the cerium center to be pseudo-octahedral, with coordination of two bidentate ligands and two monodentate ligands, in which the NHC groups are unbound, and the Ce–C_{carbene} bond lengths are 2.693(6) and 2.652(7) Å.

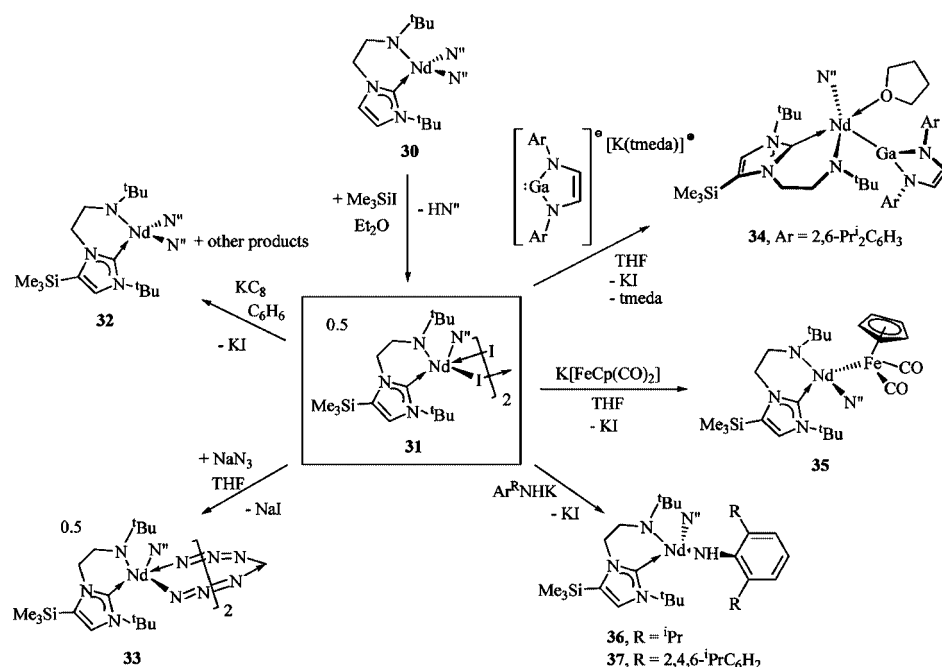
Two additional pieces of data confirm that the single crystal was representative of the diamagnetic bulk material and that the pendant NHC groups are free carbenes and not protonated imidazolium cations: First, a Ce^{III}-containing impurity from another reaction was isolated and characterized as [CeL₂(HL)₂]⁺ (**28a**) by structural characterization. This provided an analogous structure with both pendant imidazolium groups and Ce^{III}–NHC bond lengths for comparison, confirming that the NHC groups in **28** had not been protonated. Second, **28** was treated with 2 equiv of the Lewis acid 9-BBN (9-borabicyclo[3.3.1]nonane), affording the borane adduct **29** (Scheme 4). Structural characterization revealed a very similar structure to **28**, with a pseudo-octahedral geometry at the cerium center, average Ce–C_{carbene} bond lengths of 2.704(2) Å, and average B–C_{carbene} bond lengths of 1.639(3) Å.

3.3. Neodymium-NHC Complexes

There are no reported praseodymium NHC complexes.

Our group has recently reported a series of neodymium NHC complexes derived from complex **30** (Scheme 5), which was synthesized in an analogous manner to the cerium congener, **21** in Figure 6, via the reaction of NdN₃ with [(HL)•LiBr]₂ (shown in Scheme 1).³⁵ Subsequent treatment of **30** with Me₃SiI afforded **31**, as the C4-silylated iodide-bridged dimer, in an analogous fashion to **24**. Both complexes were structurally characterized; **30** is isomorphous with **21**. In **30** the neodymium center has a distorted tetrahedral geometry with a Nd–C_{carbene} bond length of 2.609(3) Å. Complex **31** is dimeric in the solid state with a central *transoid* Nd₂I₂ four membered ring, with five-coordinate neodymium centers in a distorted trigonal bipyramidal geometry. The Nd–C_{carbene} bond length of 2.656(5) Å is longer than that in **30**, which reflects the higher

Scheme 5



coordination number as well as the softer nature of the silylated NHC. In an attempt to probe the reduction chemistry of complex **31**, with the possibility of isolating an activated dinitrogen complex, it was treated with potassium graphite under a dinitrogen atmosphere, but the reaction yielded **32** in low yield as the only isolable product. This results from ligand redistribution/disproportionation and demonstrates the subtle electronic requirements for reductive activation at these metal centers. In the solid state structure of complex **32**, the neodymium center adopts a distorted tetrahedral geometry with a $\text{Nd}-\text{C}_{\text{carbene}}$ bond length of 2.648(3) Å, which is longer than that observed in **30** but the same as that in **31**, despite the larger coordination number of the metal center in this complex. The only difference between complexes **30** and **32** is the silylated C4 position in the latter, and this allows for a direct probe of the effect of incorporation of an electropositive silicon atom into the NHC σ -framework. The elongation of the $\text{Nd}-\text{C}_{\text{carbene}}$ bond length between **30** and **32** is commensurate with this.

Despite the reduction of **31** proving unsuccessful, salt elimination chemistry is facile, so that a reaction between **31** and 2 equiv of NaN_3 furnishes **33** (Scheme 5). The solid state structure reveals a $\text{Nd}-\text{C}_{\text{carbene}}$ bond length of 2.672(3) Å, longer than that in the other five-coordinate complex **31**, while the average $\text{N}-\text{N}$ bond distances of 1.16 Å are consistent with double bonds.

In pursuance of the utility of **31** in salt elimination chemistry, a reaction between **31** and the anionic gallium heterocycle $[\text{Ga}(\text{N}''\text{ArCH})_2][\text{K}(\text{tmeda})]$ ($\text{Ar} = 2,6\text{-}^i\text{Pr}_2\text{C}_6\text{H}_3$), which is valence isoelectronic with an NHC, was undertaken and yielded **34** (Scheme 5), which is also the first example of an f-element-gallium bond.³⁶ X-ray structural characterization revealed the neodymium center to be in a distorted trigonal bipyramidal geometry, with an unprecedented $\text{Nd}-\text{Ga}$ bond length of 3.2199(3) Å and a $\text{Nd}-\text{C}_{\text{carbene}}$ bond length of 2.669(2) Å, which is at the higher end of reported $\text{Nd}-\text{NHC}$ bonds and reflects the presence of the nucleophilic, anionic gallium heterocycle. A DFT study on a model of complex **34** suggested a $\text{Nd}-\text{Ga}$ bond with a small degree of covalent character.

Our group has also very recently reported complex **35**, synthesized by treatment of **31** with 1 equiv of $\text{K}[\text{CpFe}(\text{CO})_2]$ ($\text{K}[\text{Fp}]$) in THF (Scheme 5), in which the product contains an unsupported $\text{Nd}-\text{Fe}$ bond.³⁷ The ^1H NMR spectrum of **35** contains a set of paramagnetically shifted ligand resonances between $\delta = 70$ and -6 ppm and possesses a solution magnetic moment of $3.41 \mu_B$. Structural analysis reveals the geometry at the Nd cation to be distorted tetrahedral, with a $\text{Nd}-\text{Fe}$ bond length of 2.9942(7) Å and a $\text{Nd}-\text{C}_{\text{carbene}}$ bond length of 2.606(4) Å, comparable to that observed in the parent unsilylated **30**. Computational analysis indicated that the $\text{Nd}-\text{Fe}$ bond is principally ionic in character, supported by FTIR measurements which showed a shift of the asymmetric $\nu(\text{CO})_{\text{as}}$ stretch from 1770 cm^{-1} in $\text{K}[\text{Fp}]$ to 1845 cm^{-1} in **35**. The magnitude of this shift ($\delta\nu_{\text{as}}$) of 75 cm^{-1} is smaller than the ($\delta\nu_{\text{as}}$) of 146 cm^{-1} observed in $[\text{Me}(\text{CH}_2\text{SiMe}_3\text{N})_2]\text{Ti}-\text{Fp}]$, in which a significant $\text{Ti}-\text{Fe}$ π -backbonding component was ascribed.³⁸

Subsequently, treatment of **31** with potassium aryl-amides afforded complexes **36** and **37** (Scheme 5), which display dichroic behavior in solution; dilute solutions (or samples viewed through a short path length) appear pale blue, whereas more concentrated (or longer path length) solutions appear dark red.³⁹ The solid-state structures of **36** and **37** exhibit a neodymium center with distorted tetrahedral geometry and similar $\text{Nd}-\text{C}_{\text{carbene}}$ bond lengths of 2.612(4) and 2.603(6) Å, respectively, which lie at the shorter end of reported $\text{Nd}-\text{NHC}$ bonds. The $\text{Nd}-\text{NHC}$ bond in **37** is considerably more distorted from the idealized trigonal planar geometry than that in **36**, as a consequence of the much greater steric profile of the terphenyl ligand compared to the Dipp group. The “pitch” and “yaw” angles (see the Abbreviations section) in **36** and **37** are 6.5° and 4.3° and 18.0° and 0.9° , respectively. Attempts to effect a second deprotonation of the primary amide moiety to afford anionic imido species yielded only ligand exchange or decomposition products.

Very recently, Shen et al. have reported the use of a salicylaldimine-functionalized NHC ligand in the synthesis of a neodymium bis-NHC monobromide complex,

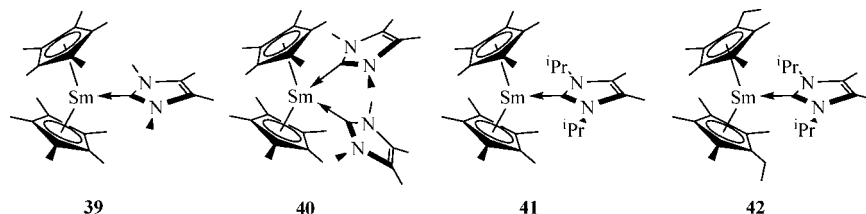
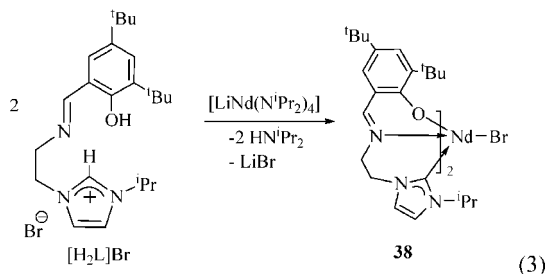


Figure 8.

L_2NdBr (**38**), in eq 3 ($\text{L} = [3,5\text{-}^t\text{Bu}_2\text{-}2\text{-(O)C}_6\text{H}_2\text{CH}=\text{NCH}_2\text{CH}_2(\text{C}\{\text{NCHCHN}^i\text{Pr}\})]$).⁴⁰



Scheme 6

This complex was accessed *via* a synthetically straightforward and useful protonolysis route involving a lanthanide amide $[\text{LiNd}(\text{N}^i\text{Pr}_2)_4]$ and 2 equiv of the imidazolium bromide ligand precursor $[\text{H}_2\text{L}]\text{Br}$, and it afforded **38** in good yield. This complex was structurally characterized and found to be monomeric and coordinatively saturated in the solid state, precluding the formation of bromide-bridged dimers that have been seen previously. The authors describe the geometry at the neodymium center as a capped octahedron with equal $\text{Nd}-\text{C}_{\text{carbene}}$ bond lengths of 2.717(3) Å, longer than those of other neodymium-NHC complexes. If the higher coordination number of Nd is taken into account, however, the ligand is deemed to enforce stronger binding of the NHC group to the Nd cation.

3.4. Samarium(II)-NHC Complexes

Divalent samarium NHC complexes were among the first examples of lanthanide-NHC complexes; all those reported to date are simple adducts of substituted samarocenes (Figure 8).

The complexes were synthesized by displacement reactions of solvated samarocenes with free carbenes, and all four depicted above were structurally characterized. A comparison of the range of complexes and the $\text{Sm}-\text{C}_{\text{carbene}}$ bond lengths observed in the solid state is displayed in Table 1.

3.5. Samarium(III)-NHC Complexes

The trivalent NHC adduct, $[(\text{C}_5\text{H}_4\text{-}^t\text{Bu})_2\text{SmCl}(\text{C}\{\text{N}^i\text{PrCMe}\}_2)]$ (**43**), was synthesized by the reaction between $[(\text{C}_5\text{H}_4\text{-}^t\text{Bu})_2\text{SmCl}]_2$ and the free carbene.⁴⁴ Structural analysis revealed a $\text{Sm}-\text{C}_{\text{carbene}}$ bond length of 2.62(2) Å, and complex **43** was evaluated as a catalyst for isoprene polymerization but proved to be almost inactive. The complex was found to be unstable in benzene solution with

respect to ligand redistribution, resulting in an equilibrium mixture of $\text{Sm}(\text{C}_5\text{H}_4\text{-}^t\text{Bu})_3$ and $[(\text{C}_5\text{H}_4\text{-}^t\text{Bu})\text{SmCl}_2(\text{C}\{\text{N}^i\text{PrCMe}\}_2)]$.

A computational analysis on the nature of the samarium-NHC bond has also been reported,⁴⁵ in which it was concluded that NHC to metal σ -donation was the main component involved in bonding, with a negligible π -component.

The amido-functionalized NHC samarium complex, **44** in Scheme 6, is synthesized in an analogous fashion to that of the yttrium, cerium, and neodymium congeners, **8** in Scheme 1, **21** in Figure 6, and **30** in Scheme 5, from a reaction between SmN''_3 and the lithium bromide amino-carbene adduct $[(\text{HL})\cdot\text{LiBr}]_2$; see Scheme 1.²² A single crystal X-ray diffraction study revealed a pseudotetrahedral geometry at the samarium center with a $\text{Sm}-\text{C}_{\text{carbene}}$ bond length of 2.588(2) Å, which is shorter than those in the examples described above. The outcome of reactions of **44** with reductants was dependent on the reductant employed.²⁴ With KC_8 reduction, a dark purple oil readily formed, characteristic of the formation of a divalent samarium species, although repeated attempts to crystallize the purple product from this failed and only decomposition products were isolated.

Brief heating of the purple reaction mixture resulted in a color change to dark red, from which **45** was crystallized as the ether cleavage product. The solid state structure is dimeric, constructed around a *transoid* Sm_2O_2 four-membered core, which is strictly planar as a consequence of residing over a crystallographic inversion center. The samarium center adopts a distorted trigonal bipyramidal geometry and displays a $\text{Sm}-\text{C}_{\text{carbene}}$ bond length of 2.682(3)

Table 1

compd	$\text{M}-\text{C}_{\text{carbene}}$ bond length (Å)	ref
39		41
40	2.837(7), 2.845(7)	41
41	2.782(3)	42
42		43

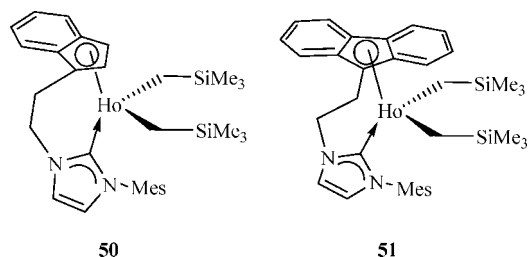


Figure 9.

Å, which is longer than that observed in **44**, a result of the higher coordination number.

Treatment of **44** with potassium naphthalenide in DME affords the bimetallic complex **46** (Scheme 6), which is analogous to the yttrium congener **9** in Scheme 2. Both complexes are isostructural in the solid state, with **46** displaying a Sm–C₄ bond length of 2.509(3) Å.

The samarium analogue of L₂NdBr (see **38** in eq 3), **47** (L = [3,5-ⁱBu₂-2-(O)C₆H₂CH=NCH₂CH₂(C{NCHC-HNⁱPr})]), was reported in the same paper, is isostructural in the solid state, and displays a Sm–C_{carbene} bond length of 2.685(6) Å.⁴⁰

3.6. Europium(III)-NHC Complexes

There are only two examples of europium NHC complexes. The first is the analogue of the yttrium complex **4** (see Figure 2), [Eu(thd)₃(C{NMeCMe}₂)] (**48**) (where thd = Bu^tC(O)CHC(O)ⁱBu), in which the europium center adopts a trigonal bipyramidal geometry and displays a Eu–C_{carbene} bond length of 2.663(4) Å.²⁰ The second example is the europium analogue of **44** in Scheme 6 (**49**) and is recorded as a private communication in the Cambridge crystallographic database (#605446). In this complex, the Eu–C_{carbene} bond length is 2.562(3) Å.

3.7. Mid-lanthanide-NHC Complexes

There are no reported gadolinium, terbium, or dysprosium NHC complexes.

3.8. Holmium(III)-NHC Complexes

The only examples of holmium NHC complexes are the bis-alkyl analogues of complexes **1** and **2** (Figure 1), bearing indenyl- and fluorenyl-functionalized NHC ligands.¹⁸ Thus, the indenyl-functionalized complex [(Ind-NHC)Ho(CH₂SiMe₃)₂] (**50**) and the fluorenyl-functionalized complex [(Flu-NHC)Ho(CH₂SiMe₃)₂] (**51**) were synthesized by *in situ* deprotonation of the corresponding imidazolium bromide precursor with LiCH₂SiMe₃, followed by addition of [Ho(CH₂SiMe₃)₃(THF)₂] (Figure 9).

The solid state structures of both complexes were determined and showed Ho–C_{carbene} bond lengths of 2.490(2) and 2.484(3) Å, respectively, where both holmium metal centers adopt a tetrahedral geometry.

3.9. Erbium(III)-NHC Complexes

Anwander et al. reported the first erbium NHC complex in 1997 as the adduct of erbium trichloride, [ErCl₃-(C{NMeCH}₂)₂]₃ (**52**), in Figure 10, although no X-ray structure was obtained.²¹ Ten years later, Schumann et al. reported mono- and bis-NHC adducts of erbium tris-alkyls, formed by solvent displacement reactions, [(Me₃SiCH₂)₃-

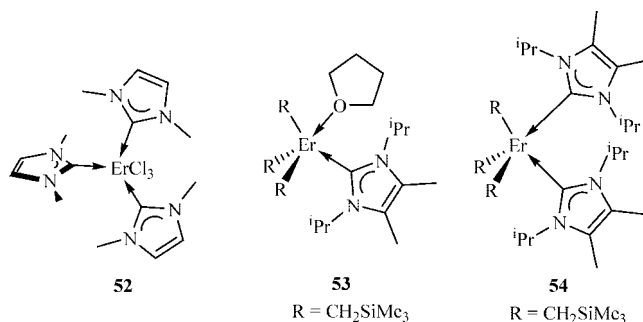


Figure 10.

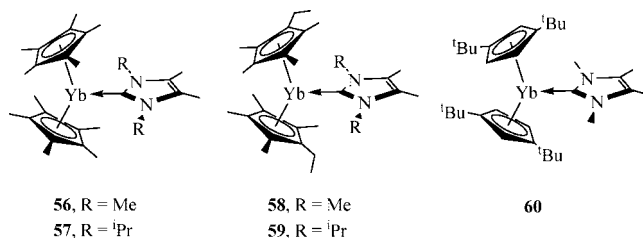


Figure 11.

Er(THF)(C{NⁱPrCMe}₂)] (**53**) and [(Me₃SiCH₂)₃-Er(C{NⁱPrCMe}₂)₂] (**54**) in Figure 10.⁴⁶ Although suitable single crystals of **54** could not be grown, the solid state structure of **53** was determined and the erbium ion was found to adopt a distorted bipyramidal geometry and displayed an Er–C_{carbene} bond length of 2.520(6) Å.

The erbium analogue of L₂NdBr (**38**) in eq 3, **55** (L = [3,5-ⁱBu₂-2-(O)C₆H₂CH=NCH₂CH₂(C{NCHC-HNⁱPr})]), was reported in the same paper. It is isostructural in the solid state, and the Er–C_{carbene} bond length is 2.568(7) Å.⁴⁰

3.10. Ytterbium(II)-NHC Complexes

As well as the samarium NHC examples, NHC adducts of substituted ytterbocenes were among the first lanthanide NHC complexes reported by Schumann et al. in 1994.^{43,47,48} A series of complexes were reported with differing substitution patterns on the cyclopentadienyl ligands or NHC N-substituents (Figure 11).

Due to the diamagnetic nature of divalent ytterbium complexes, it is possible to obtain ¹³C NMR spectral data, and these, along with the Yb–C_{carbene} bond lengths for the various complexes, are summarized in Table 2.

The NHC adducts of substituted trispyrazolylborate (Tp^{ⁱBu,Me}) supported ytterbium(II) complexes, **61** and **62**, were reported by Takats et al., *via* solvent displacement reactions.⁴⁹ Thus, **61** was formed by treatment of the corresponding THF solvate, (Tp^{ⁱBu,Me})YbI(THF) with 1 equiv of free carbene, whereas **62** was synthesized from the reaction of the THF-solvated ytterbium alkyl (Tp^{ⁱBu,Me})Yb(CH₂SiMe₃)(THF) and an excess of free carbene (Figure 12). The product is the result of both solvent displacement by the NHC and metalation of one N-Me substituent of the NHC.

Both complexes were structurally characterized, and **61** has a five coordinate ytterbium center, but with a geometry

Table 2

compd	M–C _{carbene} bond length (Å)	δ ¹³ C C _{carbene} (ppm)	ref
56		205.0	43
57		200.7	43
58	2.552(4)	205.0	47
59		198.1	47
60	2.598(3)	201.8	43

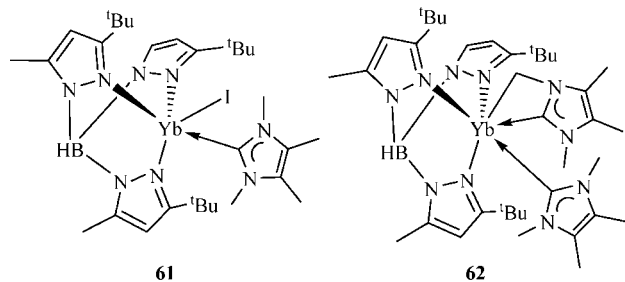


Figure 12.

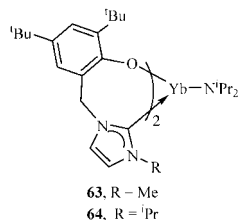


Figure 13.

closer to square pyramidal than trigonal bipyramidal, as a consequence of the distortion imposed by the tridentate Tp ligand. The Yb–C_{carbene} bond distance of 2.641(6) Å is longer than those of other divalent ytterbium examples, due to the higher degree of steric crowding at the metal center, suggesting a weaker Yb–NHC bonding interaction. The solid state structure of **62** reveals a six coordinate ytterbium center in a distorted octahedral geometry. The Yb–C_{carbene} bond lengths are 2.710(5) Å for the monodentate NHC ligand, longer than in **61** due to the higher coordination number, and 2.609(5) Å for the hydrocarbyl tethered bidentate NHC ligand, which is shorter despite this. The Yb–hydrocarbyl bond length of 2.589(5) Å is comparable to that in the ytterbium alkyl starting material, when corrected for the increase in coordination number.

The ¹³C NMR spectrum of **61** displays a C_{carbene} resonance at δ = 199.8 ppm, whereas the two C_{carbene} resonances in **62** are observed at δ = 208.3 and 201.7 ppm.

3.11. Ytterbium(III)-NHC Complexes

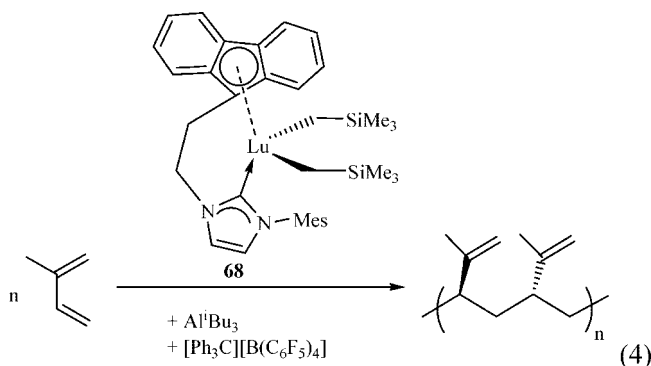
Ytterbium amide complexes bearing aryloxy-functionalized NHC ligands have been reported. A reaction between [LiYb(NⁱPr)₂]₄, 2 equiv of the corresponding imidazolium chloride salt, and 1 equiv of Li^tBu affords the bis-NHC complexes **63** and **64** in Figure 13, respectively.⁵⁰ Attempts to synthesize the mono-NHC compounds failed due to the apparent instability of the product complexes. Both complexes were structurally characterized by single crystal X-ray diffraction and found to be isostructural, with the ytterbium ion in each case adopting a distorted trigonal bipyramidal geometry. The Yb–C_{carbene} bond distances in **63** are 2.483(4) and 2.491(4) Å, which are shorter than those observed in **64** of 2.526(7) and 2.543(7) Å. This is attributable to the greater steric profile of the *N*-isopropyl group over the methyl variant. No ¹³C NMR data could be obtained for these complexes due to the paramagnetic nature of trivalent ytterbium.

3.12. Lutetium(III)-NHC Complexes

The lutetium analogues of **53** and **54** (see Figure 10) were reported by Schumann et al. at the same time as the mono- and bis-NHC adducts of lutetium tris-alkyls, formed by

solvent displacement reactions, [(Me₃SiCH₂)₃Lu(THF)(C{NⁱPrCMe}₂)₂] (**65**) and [(Me₃SiCH₂)₃-Lu(C{NⁱPrCMe}₂)₂] (**66**).⁴⁶ The solid state structure of **65** reveals a distorted bipyramidal geometry at the lutetium ion with a Lu–C_{carbene} bond length of 2.488(3) Å, shorter than that in **53** due to the decrease in size from erbium to lutetium. Complex **66** is also five coordinate in the solid state, but the geometry at the lutetium center changes to resemble a heavily distorted square pyramid, and the Lu–C_{carbene} bond lengths are significantly different at 2.557(6) and 2.639(7) Å. Only the ¹³C NMR C_{carbene} resonance for **65** was given; δ = 199.5 ppm.

The other examples of lutetium NHC complexes are the bis-alkyl analogues of complexes **1** and **2** (Figure 1), bearing indenyl- and fluorenyl-functionalized NHC ligands.¹⁸ Thus, the indenyl-functionalized complex [(Ind-NHC)Lu(CH₂SiMe₃)₂] (**67**) and the fluorenyl-functionalized complex [(Flu-NHC)Lu(CH₂SiMe₃)₂] (**68**) were synthesized by *in situ* deprotonation of the corresponding imidazolium bromide precursor with LiCH₂SiMe₃, followed by addition of [Lu(CH₂SiMe₃)₃(THF)₂]. The solid state structures of both complexes were determined and showed Lu–C_{carbene} bond lengths of 2.443(3) and 2.431(3) Å, respectively, where both lutetium metal centers adopt a tetrahedral geometry. The ¹³C NMR spectra of **67** and **68** display C_{carbene} resonances at δ = 199.9 and 199.2 ppm, respectively. Complex **68** displays 3,4-selective living polymerization of isoprene and enhanced activity and selectivity over complex **67** (eq 4).



4. Actinide-NHC Complexes

In comparison to the number of NHC complexes of late transition metals, those with Lewis acidic metal centers are much more scarce. Examples of uranium NHC complexes are no exception to this trend, with the first example being reported by Oldham in 2001.⁵¹ To date, there remain a dearth of complexes of this type in the literature.

No thorium NHC complexes have been reported to date.

4.1. Uranium(III)-NHC Complexes

All of the trivalent uranium NHC complexes, shown in Figure 14, are adducts of the simplest NHC, C-(NMeCMe)₂, which acts as a neutral two electron donor ligand. They can be synthesized by mixing the free NHC with the corresponding U^{III} starting material. Meyer et al. described complexes **69**, formed from the well-established U^{III} precursor UN³, and the tris(aryloxy)triazacyclononane **70**.⁵² Both complexes have been structurally characterized and possess U–C_{carbene} bond lengths of 2.672(5) and 2.789(14) Å, respectively. The UV–vis–NIR spectroscopic data show a bathochromic shift of an intense charge transfer (CT) band

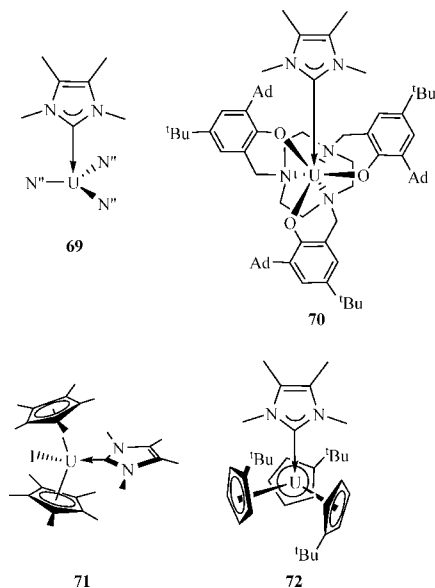


Figure 14.

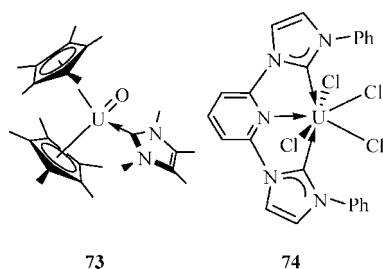


Figure 15.

in the electronic absorption spectra, from 478 to 594 nm in **69** and from 424 to 496 nm in **70**. The larger shift observed for **69** is in accordance with the shorter U–C_{carbene} bond length observed from X-ray structural analysis. Computational analysis of these complexes supported the experimental findings and suggests that there is a significant π -back-bonding component present in the NHC coordination to the electron rich U^{III} center, involving f-type uranium orbitals and π -type orbitals on the carbene ligand.

The indication of π -acceptor ability and softness of NHCs prompted Ephritikhine to demonstrate the stability of complexes **71** and **72**.³³ The U–C_{carbene} bond lengths in these complexes are 2.687(5) and 2.768(5) Å, respectively, and are comparable to those observed in complexes **69** and **70**. This was part of an investigation into the slightly enhanced covalency of the actinide 5f orbitals compared to the lanthanide 4f orbitals. Accordingly, the U^{III} complex showed a stronger interaction with the soft NHC ligand than the analogous Ce^{III} complex **25** in Figure 7. A competition reaction was used to demonstrate a slightly preferential

complexation of the carbene for U^{III} over Ce^{III}. Such demonstrations of chemical selectivity are important for the development of more effective and selective ligand sets for the partitioning of spent nuclear fuel.

4.2. Uranium(IV)-NHC Complexes

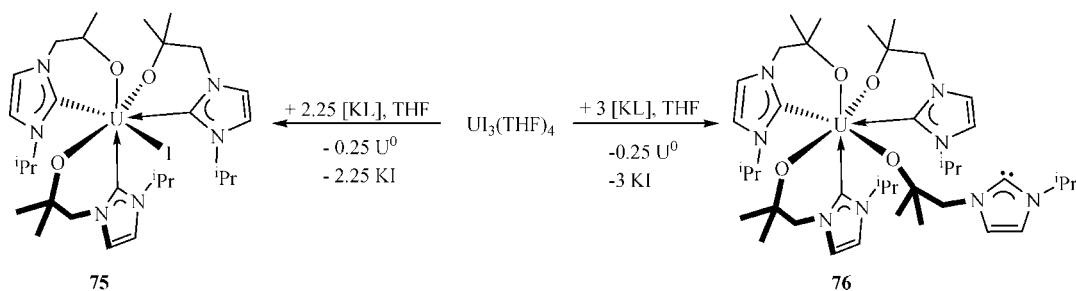
The first U^{IV}–NHC complex was reported by Evans (**73** in Figure 15) and is also a rare example of a uranium mono-oxo-compound.⁵³ This complex was synthesized *via* the reaction between [U(C₅Me₅)₃] and C(NMeCMe)₂ but was accompanied by unexpected oxidation, to give the mono-oxo-NHC complex. Little spectroscopic information is provided for this compound, but it was structurally characterized and possesses a U–C_{carbene} bond length of 2.636(9) Å and a U=O bond length of 1.916(6) Å. This was found to be shorter than that in other U^{IV} bridging oxides or terminal hydroxides but longer than that in other higher valent uranium terminal mono-oxides. Taken together, these data support the assignment of a U^{IV} terminal mono-oxide structure.

Danopoulos et al. reported a UCl₄ adduct of a pyridine-substituted dicarbene ligand (**74**).⁵⁴ Structural characterization showed the complex had U–C_{carbene} bond lengths of 2.573(5) and 2.587(5) Å, which are shorter than those in any other U–NHC complex.

We have shown that treatment of uranium triiodide with 2.25 equiv of [KL] furnishes complex **75** (Scheme 7) in high yield, although no single crystals suitable for an X-ray diffraction study could be grown and the complex was characterized by ¹H NMR spectroscopy and elemental analysis results.⁵⁵

Treatment of uranium triiodide with 3 equiv of [KL] produces the arguably more interesting **76**, which was structurally characterized and shown to have a seven-coordinate U^{IV} center with one unbound NHC group. The average U–C_{carbene} bond length of 2.747(3) Å is long compared to those of other U^{IV} NHC complexes, although it has a higher coordination number. This was the first example of a metal complex containing a free NHC group which was stable toward protonation to form the imidazolium cation. The ¹H NMR spectrum showed only two broad singlets at δ = 17 and –6 ppm but after cooling to 228 K revealed four different ligand environments, which suggested the presence of a dynamic equilibrium process between the free and bound NHC groups. Attempts were made to freeze out the fluxional process present in **76** by coordinating metal fragments such as [W(coe)(CO)₅] and [Mo(nbd)(CO)₅] (where coe = cyclooctene and nbd = norbornadiene), but due to the insoluble nature of the resulting complexes, only IR spectroscopy and elemental analyses were used to confirm their identity. Addition of BH₃·SMe₂ formed the corresponding NHC-borane adduct U(LBH₃)₄; a single crystal X-ray

Scheme 7



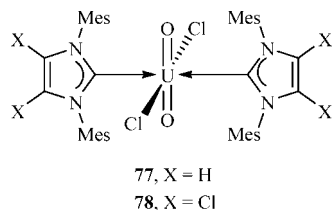
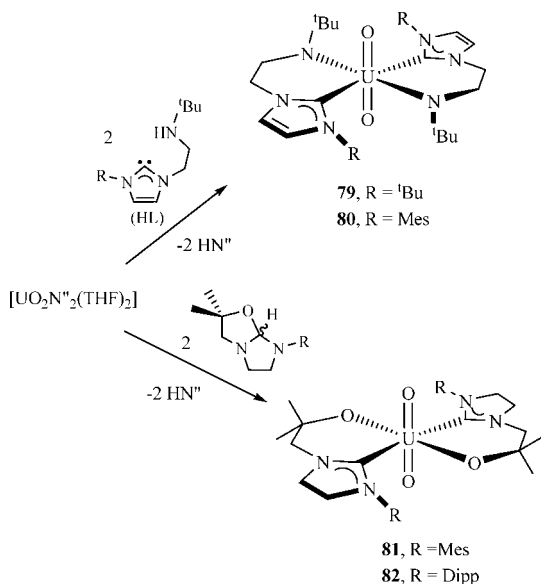


Figure 16.

Scheme 8



diffraction structural study showed the gross features of the structure to be essentially the same as those of the starting material.

4.3. Uranium(VI)-NHC Complexes

These are all adducts of the uranyl dication, $[\text{UO}_2]^{2+}$. Compounds containing a uranyl–carbon bond of any sort are scarce, and only a few uranyl–NHC complexes have been reported.

Complexes **77** and **78** (Figure 16) were the first examples of an actinide–NHC and were synthesized *via* solvent displacement in $[\text{UO}_2\text{Cl}_2(\text{THF})_3]$ with 2 equiv of the corresponding free carbene.⁵¹ X-ray structural analyses of both complexes showed the $\text{U}=\text{O}$ bond lengths to be 1.761(4) and 1.739(3) Å for **77** and **78**, respectively, which are within expected values. The $\text{U}-\text{C}_{\text{carbene}}$ bond lengths are 2.626(7) and 2.609(4) Å, which are longer than previously observed with other neutral donor ligands. The shorter $\text{U}=\text{O}$ bond length in **78** than in **77** is consistent with this NHC ligand being a comparatively weaker σ -donor, due to the σ -electron-withdrawing chlorine substituents.

The highest intensity peak in the IR spectra of **77** and **78** is assigned to the asymmetric UO_2 stretch, at 938 and 942 cm^{-1} , respectively; this frequency is inversely proportional to the donor strength of the equatorial ligands. These values are some of the highest reported compared to other neutral donor ligands and are consistent with the NHC's being poor donors to the UO_2 fragment.

We subsequently reported the second group of uranyl–NHC complexes, **79** and **80** in Scheme 8, with the NHC bearing an amido-functionalized arm.⁵⁶ These complexes can be synthesized either *via* treatment of $[\text{UO}_2\text{N}''_2(\text{THF})_2]$ with 2 equiv of amine carbene (HL) [$\text{L} = {}^t\text{BuNHCH}_2\text{CH}_2-$

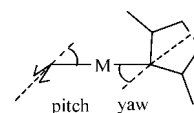
$[\text{C}({}^t\text{BuN}(\text{CHCH})\text{N})]$, see Scheme 8] or by a salt elimination reaction between $[\text{UO}_2\text{Cl}_2(\text{THF})_2]$ and 1 equiv of $[\text{LiL}]_2$. The ^{13}C NMR spectra of **79** show a very high frequency $\text{C}_{\text{carbene}}$ shift of $\delta = 262.8$ ppm, the highest so far recorded for an unsaturated–NHC–metal complex at that time. Both **79** and **80** were structurally characterized and showed the $\text{U}=\text{O}$ bond lengths to be essentially the same at 1.801(4) Å, longer than that in complex **77**, and $\text{U}-\text{C}_{\text{carbene}}$ bond lengths of 2.640(5) and 2.633(7) Å, respectively, which are only marginally longer than those observed in complexes **77** and **78**.

The UO_2 asymmetric stretch was observed in the IR spectra at 929 and 933 cm^{-1} for **79** and **80**, respectively. Each lies at a lower frequency than those observed in **77** and **78**, and this supports the longer $\text{U}=\text{O}$ bond length observed in these complexes. As the $\text{U}-\text{C}_{\text{carbene}}$ bond lengths between the two sets of complexes are very similar, the weakening of the $\text{U}=\text{O}$ bond can be attributed to the stronger donor ability of the amido substituents in **79** and **80**.

Very recently, saturated-backbone alkoxy–carbene uranyl complexes have been reported (**81** and **82** in Scheme 8) and were synthesized by treatment of $[\text{UO}_2\text{N}''_2(\text{THF})_2]$ with 2 equiv of the carbene–alcohol adduct.³¹ The ^{13}C NMR spectra of **81** and **82** show an extraordinarily high $\text{C}_{\text{carbene}}$ chemical shift of $\delta = 281.6$ and 283.6 ppm, respectively, which are the highest yet reported for a metal–NHC complex. The asymmetric UO_2 stretch in the IR spectra is observed at 851 and 853 cm^{-1} , respectively, indicating strong binding of the alkoxy–carbene ligands in the equatorial plane, resulting in weakening of the uranyl oxo bonding. Structural analysis reveals the uranyl fragment is rigorously linear and four coordinate in the equatorial plane, with symmetrical bidentate OC ligands adopting a *trans*-geometry around the metal center, enforced by a crystallographic C_2 axis. The alkoxy–carbene ligands display a bite angle of 72° , and the large aryl substituents in both complexes force the $\text{U}-\text{NHC}$ bond to tilt out of the equatorial plane, resulting in a pitch angle of 11° in **81** and 22° in **82**. The $\text{U}-\text{C}_{\text{carbene}}$ bond lengths are 2.580(4) and 2.612(2) Å, respectively, and the $\text{U}=\text{O}$ bond lengths are similar at 1.798(2) Å.

5. Abbreviations

coe	cyclooctene
Dipp	2,6- $\text{Pr}_2\text{-C}_6\text{H}_3$
Mes	2,4,6- $\text{Me}_3\text{-C}_6\text{H}_2$
N''	$\text{N}(\text{SiMe}_3)_2$
nbd	norbornadiene
NHC	N-heterocyclic carbene
thd	tetramethylheptanedioate
tmada	$\text{Me}_2\text{NCH}_2\text{CH}_2\text{NMe}_2$
pitch and yaw	terms describing the metal–NHC distortion parameters; see the drawing below



6. References

- (1) Kagan, H. B. *Chem. Rev.* **2002**, *102*, 1805. Aspinall, H. C. *Chem. Rev.* **2002**, *102*, 1807. Edelmann, F. T.; Freckmann, D. M. M.; Schumann, H. *Chem. Rev.* **2002**, *102*, 1851. Arndt, S.; Okuda, J. *Chem. Rev.* **2002**, *102*, 1953. Bochkarev, M. N. *Chem. Rev.* **2002**, *102*, 2089. Evans, W. J.; Davis, B. L. *Chem. Rev.* **2002**, *102*, 2119. Marques, N.; Sella, A.; Takats, J. *Chem. Rev.* **2002**, *102*, 2137. Molander, G. A.; Romero, J. A. C. *Chem. Rev.* **2002**, *102*, 2161. Kido, J.; Okamoto, Y. *Chem. Rev.* **2002**, *102*, 2357.

- (2) Zeimentz, P. M.; Arndt, S.; Elvidge, B. R.; Okuda, J. *Chem. Rev.* **2006**, *106*, 2404.
- (3) Nakayama, Y.; Yasuda, H. *J. Organomet. Chem.* **2004**, *689*, 4489.
- (4) Konkol, M.; Okuda, J. *Coord. Chem. Rev.* **2008**, *252*, 1577.
- (5) Boyle, T. J.; Ottley, L. A. M. *Chem. Rev.* **2008**, *108*, 1896.
- (6) Hong, S.; Marks, T. J. *Acc. Chem. Res.* **2004**, *37*, 673.
- (7) Ephritikhine, M. *Dalton Trans.* **2006**, 2501.
- (8) Evans, W. J.; Kozimor, S. A. *Coord. Chem. Rev.* **2006**, *250*, 911.
- (9) Andrea, T.; Eisen, M. S. *Chem. Soc. Rev.* **2008**, *37*, 550.
- (10) Fox, A. R.; Bart, S. C.; Meyer, K.; Cummins, C. C. *Nature (London)* **2008**, *455*, 341.
- (11) Hahn, F. E.; Jahnke, M. C. *Angew. Chem., Int. Ed. Engl.* **2008**, *47*, 3122.
- (12) Arnold, P. L.; Liddle, S. T. *Chem. Commun.* **2006**, 3959.
- (13) Liddle, S. T.; Edworthy, I. S.; Arnold, P. L. *Chem. Soc. Rev.* **2007**, *36*, 1732.
- (14) Arnold, P. L.; Pearson, S. *Coord. Chem. Rev.* **2007**, *251*, 596.
- (15) Cotton, S. A. *Lanthanide and Actinide Chemistry (Inorganic Chemistry: A Textbook Series)*; Wiley: 2006.
- (16) *The Chemistry of the Actinide and Transactinide Elements*; Springer: Dordrecht, The Netherlands, 2006.
- (17) Evans, W. J. *Inorg. Chem.* **2007**, *46*, 3435.
- (18) Wang, B. L.; Wang, D.; Cui, D. M.; Gao, W.; Tang, T.; Chen, X. S.; Jing, X. B. *Organometallics* **2007**, *26*, 3167. Wang, B.; Cui, D.; Lv, K. *Macromolecules* **2008**, *41*, 1983.
- (19) Lv, K.; Cui, D. *Organometallics* **2008**, *27*, 5438.
- (20) Arduengo, A. J., III; Tamm, M.; McLain, S. J.; Calabrese, J. C.; Davidson, F.; Marshall, W. J. *J. Am. Chem. Soc.* **1994**, *116*, 7927.
- (21) Herrmann, W. A.; Munck, F. C.; Artus, G. R. J.; Runte, O.; Anwender, R. *Organometallics* **1997**, *16*, 682.
- (22) Arnold, P. L.; Mungur, S. A.; Blake, A. J.; Wilson, C. *Angew. Chem., Int. Ed.* **2003**, *42*, 5981.
- (23) Patel, D.; Liddle, S. T.; Mungur, S. A.; Rodden, M.; Blake, A. J.; Arnold, P. L. *Chem. Commun.* **2006**, 1124.
- (24) Arnold, P. L.; Liddle, S. T. *Organometallics* **2006**, *25*, 1485.
- (25) Edworthy, I. S.; Blake, A. J.; Wilson, C.; Arnold, P. L. *Organometallics* **2007**, *26*, 3684.
- (26) Arnold, P. L.; Zlatogorsky, S.; Jones, N. A.; Carmichael, C. D.; Liddle, S. T.; Blake, A. J.; Wilson, C. *Inorg. Chem.* **2008**, *47*, 9042.
- (27) Jones, N. A.; Liddle, S. T.; Wilson, C.; Arnold, P. L. *Organometallics* **2007**, *26*, 755.
- (28) Wang, Z. G.; Sun, H. M.; Yao, H. S.; Shen, Q.; Zhang, Y. *Organometallics* **2006**, *25*, 4436.
- (29) Downing, S. P.; Danopoulos, A. A. *Organometallics* **2006**, *25*, 1337.
- (30) Downing, S. P.; Guadano, S. C.; Pugh, D.; Danopoulos, A. A.; Bellabarba, R. M.; Hanton, M.; Smith, D.; Tooze, R. P. *Organometallics* **2007**, *26*, 3762.
- (31) Arnold, P. L.; Casely, I. J.; Turner, Z. R.; Carmichael, C. D. *Chem.—Eur. J.* **2008**, *14*, 10415.
- (32) Liddle, S. T.; Arnold, P. L. *Organometallics* **2005**, *24*, 2597.
- (33) Mehdoui, T.; Berthet, J. C.; Thuery, P.; Ephritikhine, M. *Chem. Commun.* **2005**, 2860.
- (34) Casely, I. J.; Liddle, S. T.; Blake, A. J.; Wilson, C.; Arnold, P. L. *Chem. Commun.* **2007**, 5037.
- (35) Arnold, P. L.; Liddle, S. T. *Chem. Commun.* **2005**, 5638.
- (36) Arnold, P. L.; Liddle, S. T.; McMaster, J.; Jones, C.; Mills, D. P. *J. Am. Chem. Soc.* **2007**, *129*, 5360.
- (37) Arnold, P. L.; McMaster, J.; Liddle, S. T. *Chem. Commun.* **2009**, 818.
- (38) Friedrich, S.; Memmler, H.; Gade, L. H.; Li, W. S.; Scowen, I. J.; McPartlin, M.; Housecroft, C. E. *Inorg. Chem.* **1996**, *35*, 2433.
- (39) Arnold, P. L.; Liddle, S. T. *Comp. Rend. Chim.* **2008**, *11*, 603.
- (40) Zhang, J.; Yao, H.; Zhang, Y.; Sun, H.; Shen, Q. *Organometallics* **2008**, *27*, 2672.
- (41) Arduengo, A. J.; Tamm, M.; McLain, S. J.; Calabrese, J. C.; Davidson, F.; Marshall, W. J. *J. Am. Chem. Soc.* **1994**, *116*, 7927.
- (42) Glanz, M.; Dechert, S.; Schumann, H.; Wolff, D.; Springer, J. Z. *Anorg. Allg. Chem.* **2000**, *626*, 2467.
- (43) Schumann, H.; Glanz, M.; Winterfeld, J.; Hemling, H.; Kuhn, N.; Kratz, T. *Chem. Ber.* **1994**, *127*, 2369.
- (44) Baudry-Barbier, D.; Andre, N.; Dormond, A.; Pardes, C.; Richard, P.; Visseaux, M.; Zhu, C. J. *Eur. J. Inorg. Chem.* **1998**, 1721.
- (45) Maron, L.; Bourissou, D. *Organometallics* **2007**, *26*, 1100.
- (46) Schumann, H.; Freckmann, D. M. M.; Schutte, S.; Dechert, S.; Hummert, M. Z. *Anorg. Allg. Chem.* **2007**, *633*, 888.
- (47) Schumann, H.; Glanz, M.; Winterfeld, J.; Hemling, H.; Kuhn, N.; Kratz, T. *Angew. Chem., Int. Ed. Engl.* **1994**, *33*, 1733.
- (48) Schumann, H.; Glanz, M.; Gottfriedsen, J.; Dechert, S.; Wolff, D. *Pure Appl. Chem.* **2001**, *73*, 279. Fischer, R. D. *Angew. Chem., Int. Ed. Engl.* **1994**, *33*, 2165.
- (49) Ferrence, G. M.; Arduengo, A. J.; Jockisch, A.; Kim, H. J.; McDonald, R.; Takats, J. J. *Alloys Compd.* **2006**, *418*, 184.
- (50) Wang, Z. G.; Sun, H.-M.; Yao, H.-S.; Yao, Y.-M.; Shen, Q.; Zhang, Y. *J. Organomet. Chem.* **2006**, *691*, 3383.
- (51) Oldham, W. J.; Oldham, S. M.; Scott, B. L.; Abney, K. D.; Smith, W. H.; Costa, D. A. *Chem. Commun.* **2001**, 1348.
- (52) Nakai, H.; Hu, X. L.; Zakharov, L. N.; Rheingold, A. L.; Meyer, K. *Inorg. Chem.* **2004**, *43*, 855.
- (53) Evans, W. J.; Kozimor, S. A.; Ziller, J. W. *Polyhedron* **2004**, 2689.
- (54) Pugh, D.; Wright, J. A.; Freeman, S.; Danopoulos, A. A. *Dalton Trans.* **2006**, 775.
- (55) Arnold, P. L.; Blake, A. J.; Wilson, C. *Chem.—Eur. J.* **2005**, *11*, 6095.
- (56) Mungur, S. A.; Liddle, S. T.; Wilson, C.; Sarsfield, M. J.; Arnold, P. L. *Chem. Commun.* **2004**, 2738.

CR8005203